ASME-paper1

by Hariyo Pratomo

Submission date: 02-Oct-2020 08:38PM (UTC+0700)
Submission ID: 1403269194
File name: IMECE2020-23101-Pratomo.pdf (1.27M)
Word count: 6927
Character count: 36168

Proceedings of the ASME 2020
International Mechanical Engineering Congress and Exposition
IMECE2020
November 16-19, 2020, Portland, OR, USA

IMECE2020-23101

FLUID-STRUCTURE INTERACTION SIMULATION OF A BENCHMARK CONFIGURATION WITH A STRESS-BLENDED EDDY SIMULATION MODEL

Hariyo P. S. Pratomo[1]
Department of Mechanical Engineering, Petra Christian University
Surabaya, Indonesia

ABSTRACT

In this work the application of a shear stress transport based RANS-LES turbulence model on a turbulent fluid-structure interaction (FSI) benchmark is considered after a purely flow calculation over the configuration on an LES quality mesh with the hybrid modelling approach is to be performed. Within the unsteady decoupled simulation at a subcritical Reynolds number the scale resolving method successfully produces complex unsteady eddy sizes behind the reference test cube, giving a numerical Strouhal number, St of 0.184 which is close to a reference value of 0.18 from the literature. In this computation, a rubber added on the back part of a fixed circular cylinder is treated as a rigid thin plate. Furthermore, on the LES grid resolution the shielding function f_p is found to be strong to safeguard the activation of the RANS mode in the near wall region where the demarcation line between the RANS and LES areas uniquely resembles the geometry. In the FSI simulation on coarsened fluid and structural meshes with an implicit partitioned approach to couple fluid and structural solvers, the scale resolving technique successfully produces a quasi-periodic oscillating motion of the flexible structure in the first swiveling FSI mode with a corresponding Strouhal number, St_{FSI} of 0.1093 which is in a close agreement with a reference Strouhal number, St_{FSI} of 0.1128. Nevertheless, a non-physical deformation of the rubber in the spanwise direction occurs. The new FSI result is evaluated with existing results from earlier works as a pivotal basis for further investigations into applications of new mesh stiffness and subgrid-scale modelling formulations.

Keywords: arbitrary-Lagrangian Eulerian formulation, fluid-structure interaction, hybrid turbulence model, turbulent flow.

1. INTRODUCTION

Fluid-structure interaction (FSI), an interplay between fluid flow and moving or deforming solid, can be encountered in various engineering systems such as aero elasticity, airfoil mounted on wind turbine, and turbo machinery whereby the existence of turbulence within them brings additional complexity to tackle as the turbulence and deforming and moving structures interrelate reciprocally. From a numerical point of view, the simulation of such a multiphysics problem is challenging and of crucial importance in relation to the development of products or technical devices where FSI effects exist. For example, an aircraft wing designed only for the fluid flow that neglects the interaction with aerodynamic forces on the structure does not operate at its optimum in the field. With the help of FSI simulation, consequently, detailed information on structural stresses and their influence on the life span of the wing can be obtained. In principle, in the computational task of turbulent-FSI problem decisive aspects lay within coupling strategy which is to unite structural and flow software, the performance of turbulence model on moving grid, and discretization method that is to model the motion of body associated with moving numerical mesh.

Since the arrival of the Spalart-Allmaras Detached Eddy Simulation (S-A DES) in 1997 [Spalart et al 1997], nowadays various global or non-zonal hybrid RANS-LES models being capable of surmounting weakness in the accuracy of the Reynolds-averaged Navier-Stokes (RANS) simulation and the expensive computational efforts of the Large Eddy Simulation (LES) and the Direct Numerical Simulation (DNS) such as the Dynamic Hybrid RANS-LES (DHRL) [Alam et al 2017], the RANS-Implicit LES (RANS-ILES) [Islam and Thornber 2018], and the Shear Stress Transport-Stress-Blended Eddy Simulation (SST-SBES) [Ansys 2017] – only few to mention, exist. In essence, within the hybrid simulation strategies the whole boundary layer region is entrusted to RANS computation while

[1] Contact author: hariyo_p@petra.ac.id

detached flow region is assigned to LES like mode by a hybrid function where its proper functionality depends on the numerical grid resolution. Furthermore, the non-zonal hybrid turbulence modeling group does not require the users to locate LES and RANS regions separately in the computational domain prior to the execution of simulation; thus making the models straightforward for use.

SST-SBES is a new variant in the Delayed Detached Eddy Simulation (DDES) technology in the sense that it uses a new way in blending RANS and LES strategies to reduce the eddy-viscosity μ_t (in the context of the present study) via a strong shielding function f_p [Menter 2016] instead of modifying the dissipation term ε in transport equation of the turbulence kinetic energy k as performed in the DDES method. In this way, the reduced eddy-viscosity μ_t produced by SST-SBES acts to represent realistic and complex momentum transfer in the detached flow region associated with a rapid transition from RANS to LES solution. In this present paper the hybrid technique combines SST and Wall-Adapted Local Eddy-viscosity (WALE) LES models. The urgency of WALE-LES employed in SST-SBES is explained in Section 2.

All those three non-zonal hybrid turbulence formulations, i.e. SST-SBES, RANS-ILES, and DHRL are young, and have their own distinguished strategies. The key element in SST-SBES is the asymptotic or strong shielding function f_p which is exactly the same with one in the Shielded Detached Eddy Simulation (SDES) [Ansys 2017, Menter 2016]. It is the shielding function f_p which is to amalgamate existing RANS and LES proposals in SBES, and without this SBES will not be able to improve the DDES formulation; thus giving the decreased or more realistic eddy-viscosity μ_t and the fast transition to LES solution [Menter 2016]. The scenario in RANS-ILES is rather different as compared to SBES. RANS-ILES unites an enhanced Spalart-Allmaras RANS model and an ILES strategy tested in Drikakis et al (2009) instead of the WALE-LES procedure of Nicoud and Ducros (1999) in SBES and is a continuous approach with a hybrid blending function operating at the edge of boundary layers and separated flow regions [Islam and Thornber 2018]. Besides, the algorithm is informed by an auxiliary transport variable and defines a new cell size or filter width Δ and novel effective eddy-viscosity $\mu_{t,eff}$ [Islam and Thornber 2018]. Unlike RANS-ILES and DES family, DHRL, by design, is a modular approach that allows the coupling of any RANS technique with any LES model as in SBES and does not incorporate the local grid size Δ as a model variable in its governing equation [Alam et al 2017]. In the literature, however the scientists focused on the integration of the SST model and monotonically integrated LES (MILES) methodology of Fureby and Grinstein (1999). The proper activation of the RANS and LES modes is facilitated via a blending method in DHRL enforced through the assumption of continuity in total turbulence energy production, manifested by a parameter that accounts for resolved turbulence, RANS, and inhomogeneous Sub-Grid Scale (SGS) productions [Alam et al 2017]. With the knowledge, SST-SBES, as a result, is applied in this study in the contexts of stationary and moving meshes. In addition, it is encouraging for future research to unite other available RANS and LES models for SBES via the shielding function f_p where a great care must be taken with respect to the limitations of targeted RANS and LES formulations.

A turbulent-FSI benchmark consisting of a fixed circular cylinder with a rubber attached at the rear of the front body immersed in a subcritical Reynolds number-turbulent flow is proposed by De Nayer et al as a validation tool for the performance of scale resolving schemes. In the past, investigations into the performance of the scale resolving proposals on the FSI configuration of De Nayer et al were still limited to the applications of the Smagorinsky LES model of Smagorinsky (1963) in De Nayer et al, the k-ε-ζ-f DDES model of Reimann (2013) in Ali (2017), and k-ε and ζ-f based-Very Large Eddy Simulation (VLES) formulations of Kondratyuk (2017) to predict the quasi-periodic motion of the rubber in the first swiveling FSI mode. Even though the FSI test case is simple in geometry, in principle with the imposed Reynolds number it demonstrates transition in shear layers (close to the apex of the cylinder) and wake region which in turn leads to the oscillation of the rubber. On the similar test case with the same non-dimensional parameters explained in Table 1 but the rubber was replaced by a rigid plate, the existences of the transition in shear layers and the wake region were confirmed by an experimental study of Apelt and West (1975).

In the mentioned turbulent-FSI studies [De Nayer et al, Ali 2017, Kondratyuk 2017], implicit partitioned method which is to couple structural and flow solvers and the arbitrary Lagrangian Eulerian (ALE)-discretization technique were employed. It is seen that the LES, DDES, and VLES models demonstrated their performances with a varying degree of success in the multiphysics computations. The Strouhal number St_{FSI} of the rubber oscillation and the averaged-maximum and minimum values of the rubber deflection predicted by the Smagorinsky LES formulation are close to reference values in experimentation [De Nayer et al]. Nevertheless, under-predictions of the rubber oscillation occurred in the studies of Ali (2017) and Kondratyuk (2017) when coarse fluid meshes designed for URANS simulation were exercised in the coupled computations with DDES and VLES techniques. Interestingly, what is critical in the multiphysics calculations of Ali (2017) and Kondratyuk (2017) is that non-standard-filter widths Δ_{vol} are found to be more accurate than standard-filter width Δ_{max}, as explained by Kondratyuk (2017). For that reason, it is of crucial importance to expand the application of different hybrid turbulence modeling schemes to the turbulent-FSI test case in order to study their potentials and for the development of the modeling approach in the context of FSI.

SST-SBES of Ansys (2017) is considered for the simulation of the turbulent-FSI benchmark of De Nayer et al in this paper. Due to the physical nature of moving and deforming structure existing in the coupled problem which is handled by the integration of fluid solver with structural software, the implicit partitioned technique is also used in this new study as in the aforementioned turbulent-FSI works. This is aiming at

investigating the capability of SST-SBES for turbulent-FSI computation. The turbulent FSI calculation with SST-SBES is performed after a transient pure flow simulation with the global hybrid RANS-LES scheme on an LES quality mesh is concluded. The decoupled computation of the turbulent flow on the very fine grid with SST-SBES aims at richer turbulence content and testing the superiority of the shielding formulation f_p which is proprietary by Ansys.

2. MATERIALS AND METHODS

The SBES technology of Ansys (2017) is a novel but more modular and economical computation approach in DDES family, and by design the method can be run safely in DES mode with a strong shielding function f_p [Menter 2016]. In principle, the hybrid strategy is an extension of SDES in the sense that the same shielding function f_p of SDES is employed in the SBES technique but the way to arrive at a reduced eddy-viscosity μ_t to capture complex turbulence energy transfer manifested through providing fast LES solution is different in comparison to the common methodology of DDES family. As eddy-viscosity based RANS and LES methods, i.e. the SST and WALE models are united in SBES for the present study, its formulation is performed on the eddy-viscosity level as in the following expression.

$$\mu_t^{SBES} = f_p \mu_t^{SST} + (1 - f_p)\mu_t^{WALE-LES} \qquad (1)$$

Obviously, from the above equation in regions where $f_p = 1$ the SST model of Menter (1994) is authorized, and vice versa it holds for regions where $f_p = 0$, meaning that the WALE model is active. Further, the use of the WALE formulation of Nicoud and Ducros (1999) in SBES would make the methodology more superior than other DES variants to resolve turbulence scales as the WALE approach accounts for both the strain rate and the vorticity which contain turbulence energy. Accordingly, such an LES method suggests a better SGS model.

With the modeling technique, SST-SBES provides improved asymptotic protection of the boundary layer region, clear distinction between SST and WALE-LES regions based on the shielding function value, and fast transition to 3D turbulence length scales-LES solution. Additionally, the definition of the length scale in the LES mode, i.e. the SBES grid spacing Δ_{SBES} multiplied with the SBES model coefficient C_{SBES} leads to a significant reduction in the eddy-viscosity μ_t for SBES compared to other DES versions. All of these advantages are beneficial for turbulent-FSI computation which requires turbulence scales interacting with moving and/ or deforming solid, rather than the averaged-length scale supplied by any RANS procedures.

Flow parameters in the FSI benchmark of De Nayer et al include the inflow velocity U_{inflow}, flow density ρ_{fluid} and flow dynamic viscosity μ_{fluid} of 1.385 m/s, 1000 kg/m^3, and 1.0x10^{-3} Pa.s, respectively. This settles the turbulent flow over the geometry in a subcritical condition with the Reynolds number Re of 30,470. Moreover, structure parameters for the rubber have the density ρ_{rubber}, Young's modulus E, and Poissons's ratio υ of 1360 kg/m^3, 16 x 10^6 Pa, and 0.48, respectively.

Before performing the multiphysics simulation with SST-SBES, mesh convergence and time sensitivity analyses of transient flow computation with SST-RANS model are to be concluded. Afterwards, the fluid computational domain is extended into the spanwise direction to arrive at a subset domain for an unsteady flow computation with SST-SBES on an LES quality mesh. Within the decoupled computations, the rubber is treated as a rigid thin plate, and the Strouhal number St is calculated. From the optimum coarsened fluid mesh on the lateral surface established in the first step, transient computations proceed with the turbulent-FSI case with SST and SST-SBES models. The lateral surface is depicted on Figure 1. Within the turbulent-FSI computations, mesh size in the spanwise direction has only 1 cell for the RANS technique - thus having a thin computational domain while the subset domain for SST-SBES has 36 equidistant cells in the same direction. The fluid domain applies structured hexahedral mesh which is illustrated in Figure 1.

Preprocessing of the structural side for the rubber follows Kalmbach (2015). The rubber computational domain exercises a second order accurate SOLID186-brick element which is defined by 20 nodes, having three degrees of freedom per node. Triquadratic shape functions are integrated in the mesh element. As physical phenomenon in the oscillating motion of the rubber reflects moderate deformations of the flexible structure [De Nayer et al], the rubber is modeled as non-linear problem which is iteratively solved by the Newton-Raphson methodology. Within the SOLID186 element, an element technology of uniform reduced integration method is ingrained in the element type in order to prevent locking phenomena in the nearly incompressible and bending-dominated rubber where the integration technique is defined as a mixed u/P formulation. This is to circumvent complications due to incompressibility effect caused by the specified value of the Poisson's ratio.

The implicit partitioned procedure or iteratively staggered coupling scheme for the current FSI simulations is realized via the MFX interface of Ansys. The coupling strategy is to unite the Mechanical-structural and CFX-flow solvers for the coupled computations through a progression of multi-fields timesteps where each of which consists of one or more staggered or FSI iterations. Within every FSI iteration, each field solver gathers the data it requires from the other solver and solves its field equations for the current multi-field timestep. The staggered iteration is repeated within every timestep until a maximum number of FSI iterations is reached, or until the data transferred between the solvers and all field equations have converged. The converged FSI solutions within every timestep are ensured by a constant under-relaxation factor of 0.1 for the transferred force to the structural solver. With the under-relaxation coefficient, the coupled computations run stably until specified total times of simulation are reached.

Mesh movement in the FSI computations is modelled by a mesh stiffness equation relying on a hyperbolic function which is dependent on the wall distance h(**x**). The stiffness model $\zeta(x)$

applies a formulation proposed by Kalmbach (2015). The following formula defines the mesh stiffness methodology.

$$\zeta(x) = \left(\frac{1}{h(x)}\right)^{c} \quad (2)$$

With equation (2), the mesh stiffness is exponentially increased as the distance of wall h(**x**) from the nearest boundary gradually decreases. Conceptually, how strong the increase in the mesh stiffness can occur is controlled by the model exponent c which can be set in a range of 0.7 – 0.9 according to Kalmbach (2015). In this study, c is given a value of 0.9. In the future it is therefore encouraging to test other values of the exponent c within the given margin. The procedure achieves its fullness to model moving mesh after the stiffness model $\zeta(x)$ is substituted into the equation of mesh movement [Ansys 2017] as in:

$$\nabla.(\zeta(x)\nabla\Delta r_{mesh}) = 0 \quad (3)$$

where Δr_{mesh} is the relative grid displacements at each FSI iteration.

Within the turbulent-multiphysics computations with SST and SST-SBES, boundary conditions of the flow domain include inlet, outlet, no-slip wall, FSI interface, slip wall, symmetry, and periodicity while the structural part applies fixed support-, FSI interface-, and frictionless support-boundary conditions. The inlet uses RANS turbulence conditions which is defined as low turbulence intensity and eddy-viscosity ratio. On the surface of the fixed cylinder the no-slip wall is functioned. As the rubber manifests the interplay between fluid in motion and deforming solid, therefore the upper, lower, and free surfaces of the elastic structure are identified as the FSI interface. The slip wall boundary conditions are authorized to the upper and lower walls. When the RANS model is employed, the lateral walls are established to symmetry boundary conditions. However, this is not the case for the coupled simulation with SST-SBES where periodicity boundary conditions replace the symmetry conditions for the same walls. To the structural domain, the fixed support is set to the front surface of the rubber which is the surface where the pliable component is attached to the back of the fixed cylinder while the FSI interface identifies the upper, lower, back surfaces of the elastic solid. The left and right lateral surfaces of the rubber are determined as the frictionless supports. During the coupled simulations, an implicit time marching approach i.e. the second order backward Euler method facilitated by Ansys CFX is applied in the fluid domain and an extended Newmark methodology, i.e. the generalized Hilber-Hughes-Taylor (HHT)-α algorithm available in Ansys Mechanical is used in the structural counterpart, both of which are for the time integration to achieve stability.

3. RESULTS AND DISCUSSION

The transient pure flow computation with SST-SBES of Ansys (2017) is performed on the subset domain with an LES quality mesh of 14,394,528 control volumes as two-point correlations dropped towards zero value [De Nayer et al]. The fine mesh has 199,924 elements on the x-y plane and 72 equidistant cells in the z-direction. This subset domain was also used by Ali (2017) and Kondratyuk (2017). The LES grid has the properties of $\Delta y^+ < 5$, $\Delta x^+ = 40$, $\Delta z^+ = 64$, and growth rate = 1.05. Figure 1 illustrates the LES quality mesh. This mesh is to test whether or not the SBES shielding function f_p is safe to protect the RANS mode within the near wall region.

Figure 2 shows the procedure of the transient run with SBES. As shown in Figure 2 (a), two monitoring points for the turbulent kinetic energy k are added in the wake region behind the circular cylinder. The evolution in time of the turbulent kinetic energy k for the requirement of non-dimensional advection time, defined as $\{(t.U_{inflow})/D\} > 100$ is depicted in Figure 2 (b). After the t* requirement is accomplished, the statistics averaging procedure is carried out within the non-dimensional convection time of 200 to gauge the frequency f of velocity with the Fast Fourier Transform (FFT). With this, the Strouhal number St defined as $(f.D)/U_{inflow}$ is evaluated and compared with a reference value from an experiment of Apelt and West (1975). In this study, D in the Strouhal number equation is diameter of the circular cylinder. A monitoring point for the velocity is located on a middle plane of the computational domain in the wake region.

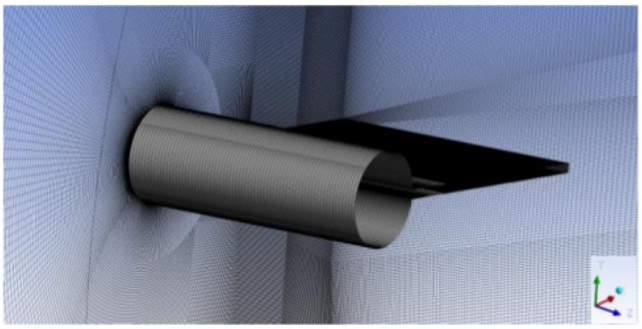

FIGURE 1: LES QUALITY MESH FOR TRANSIENT FLOW SIMULATION WITH SST-SBES. THE X-Y PLANE IS LATERAL SURFACE AND THE Z-DIRECTION REFLECTS THE SPANWISE DIRECTION.

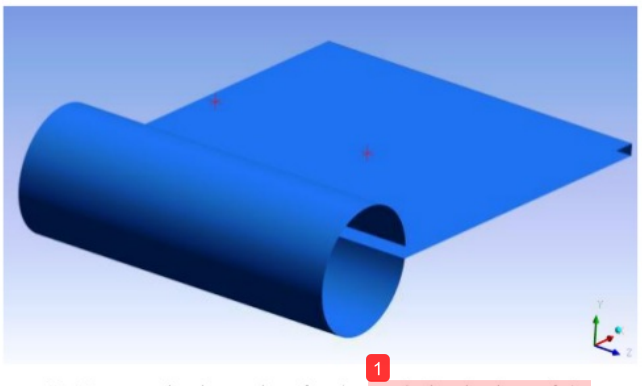

(a) Two monitoring points for the evolution in time of the turbulent kinetic energy k

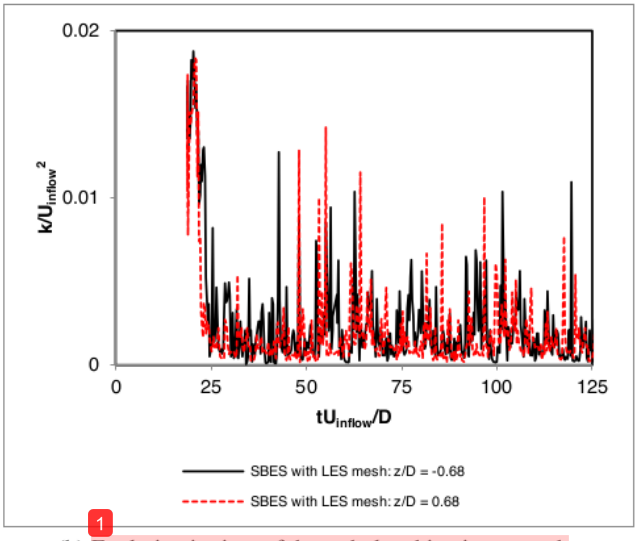

(b) Evolution in time of the turbulent kinetic energy k

FIGURE 2: PROCEDURE OF TRANSIENT FLOW COMPUTATION WITH SST-SBES ON AN LES QUALITY MESH

For the discretization of the advection or convection term, the Bounded Central Difference (BCD) scheme is employed in the SST-SBES computation. The BCD approach is numerically less dissipative than the Second Order Upwind scheme with a blending factor, i.e. the High-Resolution technique developed for the RANS calculation but is more dissipative than the Central Difference (CD) method. Nevertheless, the BCD strategy is stable and, for that reason is frequently the most favorable choice. With the BCD formulation, the Courant-Friedrichs-Lewy (CFL) condition is kept to be equal to unity, thus giving a fine timestep size Δt of 2.5 x 10^{-5} seconds for the pure flow simulation with SST-SBES.

Figure 3 (a) illustrates the visual inspection of vorticity scales over which is predicted by SST-SBES on the LES quality mesh. The turbulence scales are captured with the use of the Q-criterion at the advection time t^* of 125 after the settlement phase, i.e. $\{(t.U_{inflow})/D\} > 100$. It is clearly seen that SST-SBES successfully resolves the eddy scales on the configuration. In particular, the existence of the rigid thin plate does not suppress strong global instability associated with a wide range of the turbulence scales behind the geometry. This behavior was also revealed by Apelt and West (1975) on the same object with the similar values of non-dimensional geometrical data, i.e. L/D and h/D, submerged in the subcritical Reynolds number-flow. What is important here is that the turbulence modeling technique can demonstrate the transition in shear layers near the apex of the cylinder as also experimentally visualized by Apelt and West (1975). Nonetheless, the transition in shear layers can not be reproduced by SST-DDES, a variant of non-zonal hybrid RANS-LES model in DES family, in the same flow simulation. To this, the readers are referred to Pratomo (2020). As the modeling strategy ingrained in SST-SBES and SST-DDES as well as their paradigm is different, there is no reason to expect that SST-DDES will perform better than SST-SBES. Conceptually, in the LES mode SST-DDES is the same as SST-DES, and its eddy-viscosity obeys the Smagorinsky model recipe only under the assumption of the local equilibrium of turbulence, that is, the production rate is equal with the dissipation rate. In this way, SST-DDES in the LES mode is not identical to the Smagorinsky model or to any other algebraic LES formulation. All of these are due to the uncertainty of the local equilibrium assumption. Evidently, this was one of the reasons for the development of the SBES technology of Ansys (2017), which is able to algebraically change in the LES mode to a clearly defined LES proposal via the shielding function f_p. In SST-SBES, the hybrid modeling technique utilizes the WALE-LES model with the more superior SGS model as explained in Section 2. Another crucial aspect in SST-SBES is the new definition of the length scale in the LES mode, which leads to more realistically reduced eddy-viscosity. On top of that, the turbulence energy spectrum calculated by SST-SBES is shown in Figure 3 (b) where the dashed line represents the -5/3 inertial sub range. The spectrum is achieved from an estimate of the sub-grid (modelled) turbulent kinetic energy for the WALE-LES methodology utilized in SST-SBES where a coefficient of proportionality, i.e. dynamic model coefficient, is employed.

Tabel 1 recapitulates the Strouhal number St calculated by SST-SBES in the transient flow simulation on the LES grid. It is seen that the hybrid RANS-LES scheme performs well in the decoupled computation, giving the Strouhal number of 0.184 that is close to the reference value of Apelt and West (1975) with a relative error of 2.22%. Furthermore, what is important within the hybrid modelling strategy is the distribution of the shielding function f_p as depicted in Figure 4. It is revealed that the demarcation line between the k-ω SST and WALE-LES modes uniquely resembles the geometry. This is also found by Xie et al (2020) on a dimpled wall. The demarcation line of the distribution as seen in Figure 4 reflects the activations of the RANS procedure in the whole near-wall location colored with red (f_p = 1) and the LES methodology in the outside region colored with blue (f_p = 0). With this, an attack of the Grid Induced Separation (GIS) can be evaded. Even though the ratio of the maximum grid length along the geometry, h_{max} to the boundary layer thickness, δ is crafted to be less than 0.5 – 1 on account of the LES quality mesh, the protection function f_p remains strong to shield the boundary layer region.

The mesh convergence study on the thin computational domain with the k-ω SST model are summarized in Table 2. A timestep size Δt of 1.25 x 10^{-4} seconds is exploited in the first step. The readers are referred to Pratomo (2020) for further details on the refinement factor r, solution difference ε, convergence order p, extrapolated value ϕ, approximated relative error e_a, Grid Convergence Index (GCI), and time sensitivity analysis. The design of fluid mesh on the subset and thin domains for the multiphysics simulations is based on the convergence study. The size of the fluid mesh on the x-y plane exploited for the current FSI computations is 97,674 control volumes while Ali (2017) and Kondratyuk (2017) exercised the fluid grid size

of 54,676 control volumes in their FSI simulations with the DDES and VLES technologies. With the optimum mesh size of 97,674 control volumes, the second step proceeds with the time sensitivity analysis on the thin fluid domain with the k-ω SST model of Menter (1994). It is concluded that a timestep size Δt of 0.001 seconds is the optimal value as also tested by Kalmbach (2015). The same timestep size Δt is suited for the pure structural computation [Kalmbach 2015].

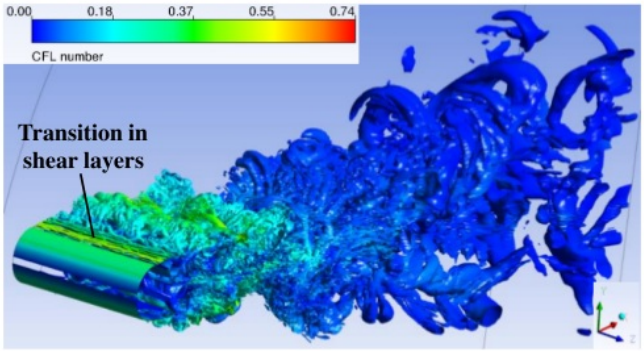

(a) Turbulence scales with Q-criterion

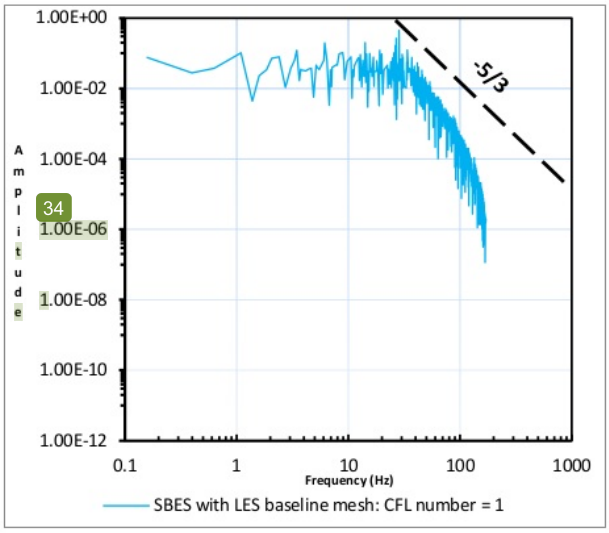

(b) Turbulence energy spectrum

FIGURE 3: TRANSIENT FLOW COMPUTATION WITH SST-SBES ON AN LES QUALITY MESH WITH CFL NUMBER OF LESS THAN 1

The transient FSI simulations with the RANS and hybrid RANS-LES procedures on the FSI benchmark of De Nayer et al are started from a symmetrical position of the rubber without the use of material damping. As 36 equidistant cells are used in the spanwise direction, the fluid mesh for SST-SBES sizes 3,516,264 control volumes while the fluid mesh for SST has only 97,674 control volumes. Compared to the current fluid mesh size for SST-SBES, a fluid mesh of 1,968,336 control volumes was applied by Ali (2017) and Kondratyuk (2017) for the DDES and VLES strategies. Additionally, the elastic structural part is discretized with (72 x 4 x 1) elements for the RANS simulation and (72 x 4 x 8) elements for the hybrid turbulence computation where the second order SOLID 186 is chosen for the mesh type. The rubber cell size in the spanwise direction manifested in the 8 cells is made equidistant, and the number of cell is sufficient as the rubber deflection in the spanwise direction does not occur [Ali 2017, Kondratyuk 2017]. With this knowledge, one monitoring point for the rubber deflection therefore is added at the middle location on the rubber free surface. Ali (2017) and Kondratyuk (2017) also used one monitoring point for the rubber deflection.

Table 1. Comparison of the Strouhal number St between the present study and experimental reference of Apelt and West (1975)

Parameter	**Numerical result with SST-SBES on LES quality mesh (h/D) = 0.09 (L/D) = 2.72**	**Apelt and West (1975) (h/D) = 0.09 (L/D) = 2.72**
Strouhal number St	0.184	0.18

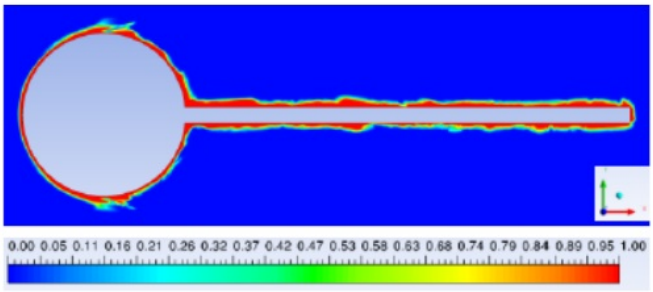

FIGURE 4: SHIELDING FUNCTION OF SST-SBES IN LATERAL MIDDLE PLANE

Table 2. Mesh independence study with the SST model.

Mesh size on x-y plane (control volume)	**Grid size h (m)**	**Strouhal number St**
23,250	0.0024	-
47,670	0.0019	0.232
97,674	0.0015	0.238
199,924	0.0012	0.241

Figure 5 (a) illustrates the flow streamlines predicted in the multiphysics computation with the SST model and captured at a certain time after the quasi-periodic oscillation of the rubber is achieved while in Figure 5 (b) the time history of dimensionless y-displacement of the rubber deflection predicted by the RANS

methodology is depicted. Within the period of simulation, it is seen that the rubber quasi-periodically oscillates. The data is then processed via the phase-averaging method to arrive at the maximum and minimum averaged-values of the deflections in the y-direction. The readers are referred to Kalmbach (2015) for the detailed procedure in the averaging technique.

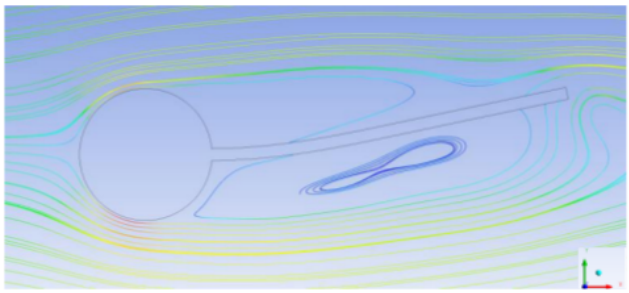

(a) Flow streamlines

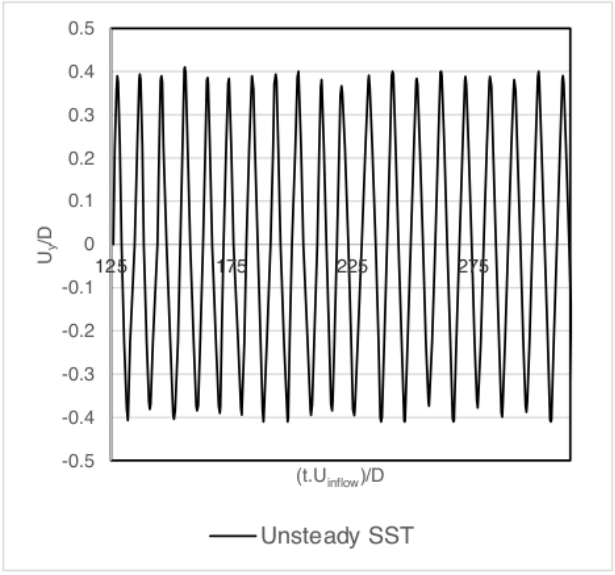

(b) Time history of dimensionless y-displacement of the structural deflection

FIGURE 5: TRANSIENT FSI SIMULATION WITH SST MODEL ON COARSENED FLUID AND STRUCTURAL MESHES

The coupled computation with SST-SBES on the coarsened fluid and structural meshes reproduces a quasi-periodic deflection in the y-direction of the elastic structure within the period of simulation, as illustrated in Figure 6. Compilation of the present and earlier FSI results is presented in Table 3. All the data are processed through the implementation of the phase-averaging procedure. In Figure 7, the averaged y-displacement predicted by SST-SBES is compared with one from the experiment of De Nayer et al.

Comparing the present FSI results with those of De Nayer et al, Kalmbach (2015), Ali (2017), and Kondratyuk (2017), it is of importance to improve the current results. It is seen that the maximum and minimum values of the rubber deflection are still below the reference values in the experiment. Because of the specified value of the exponent c, the oscillating motion of the rubber seems to be slightly dampened. To this, an encouraging solution is the implementation of a different mesh stiffness expression with different exponent values c. The readers are referred to equation (2) for the formulation of the mesh stiffness model. Alternatively, it is also possible to propose other mesh stiffness expressions which are based on the wall distance h(**x**). The mesh resolution is not the issue as the Strouhal number St is already within the asymptotic range of the convergence as can be seen in Table 2. Further, the oscillation frequency f_{FSI} of 6.74 Hz predicted by the SST model is only little different to the oscillation frequency f_{FSI} of 6.77 Hz [Kalmbach 2015]. This is owing to the coarsened fluid mesh used. Kalmbach (2015) implemented a much finer fluid mesh, even greater than 199,924 elements on the x-y plane for the coupled computation with SST.

Table 3. Summary of the present and earlier turbulent-FSI results

	f_{FSI} (Hz)	Err. (%)	$U_y^*\|max$	Err. (%)	$U_y^*\|min$	Err. (%)
Experiment [De Nayer et al]	7.10	-	0.418	-	-0.420	-
Smagorinsky LES [De Nayer et al]	7.08	0.28	0.456	9.1	-0.4.64	-10.6
SST [Kalmbach 2015]	6.77	-4.65	0.420	0.48	-0.418	0.48
SST Present study	6.74	-5.07	0.389	-6.94	-0.394	6.19
SST-SBES Present study	6.88	-3.1	0.367	-12.2	-0.372	11.43
DDES [Ali 2017]	6.97	-1.83	0.381	-8.85	-0.382	9.05
k-ε VLES [Kondratyuk 2017]	6.98	-1.69	0.374	-10.5	-0.35	-16.2
ζ-f VLES [Kondratyuk 2017]	6.99	-1.55	0.369	-11.72	-0.37	-11.9

As can be seen in Table 3, the FSI results of the present study, Ali (2017), and Kondratyuk (2017), underestimate the reference data. In particular, the maximum and minimum averaged-values of the deflection in the y-direction predicted by the non-zonal scale resolving scheme are below the values in the experiment. To the results of Ali (2017) and Kondratyuk (2017), this can be contributed to the inherent strategies in the DDES and VLES models, coarsened fluid mesh, and different mesh movement-modelling technique employed in their computation. VLES is an amalgamation procedure of RANS with DNS, which depends on the numerical mesh resolution. The detail in VLES is not discussed here as the present paper focuses on non-zonal hybrid RANS-LES approach. Unlike SBES, DDES is an old form of blending RANS and LES like modes with the modification of RANS length scale and the inclusion of shielding function to protect the near-wall region. With the paradigm,

therefore one can not expect the existence of an LES model in DDES; only LES like mode. SBES is different; there is an LES model in the new technology through the functionality of the new shielding function f_p - not just an LES like mode as in DDES proposal. With respect to this, SBES should perform better than DDES. Even so, that is not the case in the current FSI computation with SST-SBES. A compromising timestep size Δt of 5 x 10^{-4} seconds is used in the present coupled simulation.

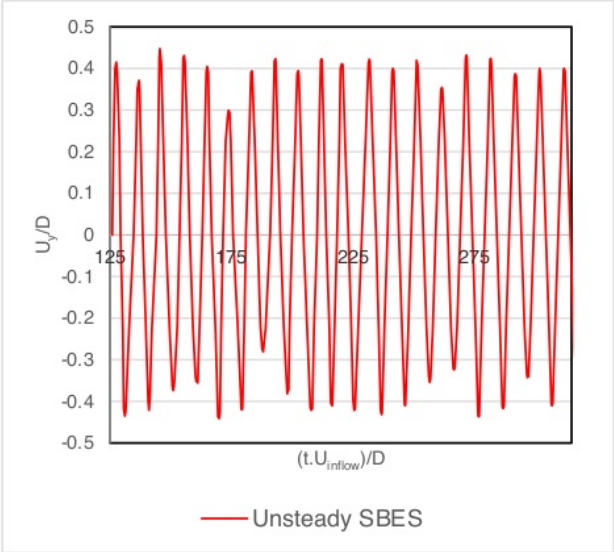

(a) Time history of dimensionless y-displacement of the structural deflection

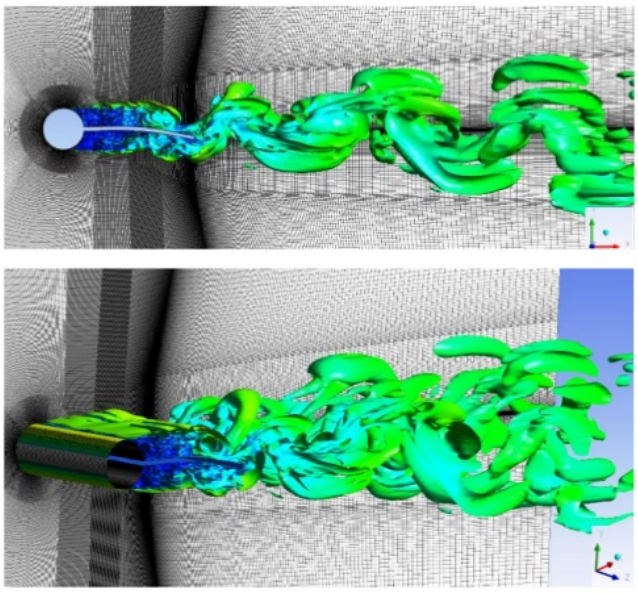

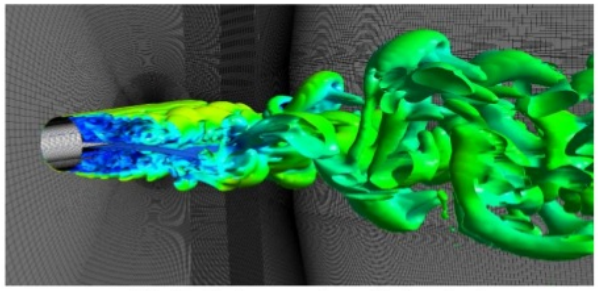

(b) Turbulence scales with Q-criterion

FIGURE 6: TRANSIENT FSI COMPUTATION WITH SST-SBES

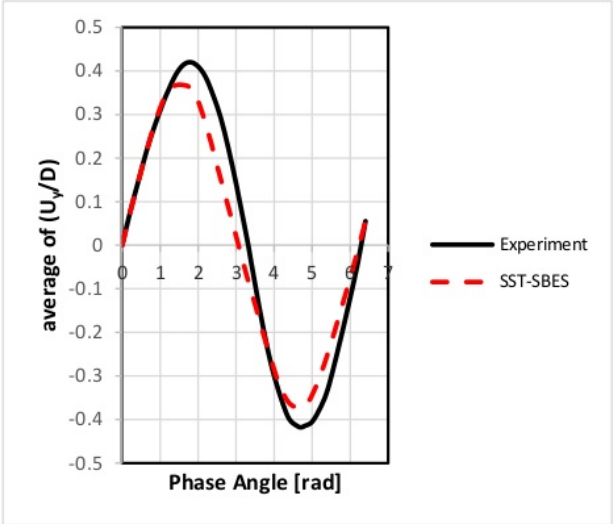

FIGURE 6: AVERAGED Y-DISPLACEMENT COMPARISON BETWEEN TURBULENT-FSI RESULTS OF SST-SBES AND EXPERIMENT

Figure 8 shows the distribution of the shielding function f_p in the SST-SBES technology located on the middle lateral plane. The protection function f_p performs well to safeguard correct operations of SST and WALE-LES computations in desired regions. As appeared in the flow computation, the demarcation line generated by the shielding function f_p of SST-SBES entirely takes after the FSI configuration. However an unphysical deformation of the rubber in the spanwise direction appears, as shown in Figure 9. Although such a problem is not expected, the shielding function f_p is safe during this challenging simulation. The non-physical deformation is presumably caused by the mesh stiffness model implemented in which its strategy is problematic in controlling the mesh stiffness in the spanwise direction as the rubber interacts with the complex turbulence scales modelled by SST-SBES.

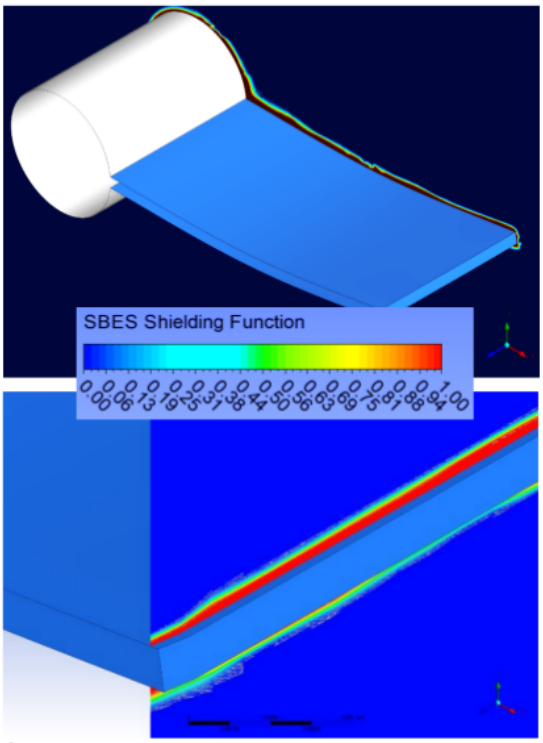

FIGURE 8: DISTRIBUTION OF SHIELDING FUNCTION OF SST-SBES

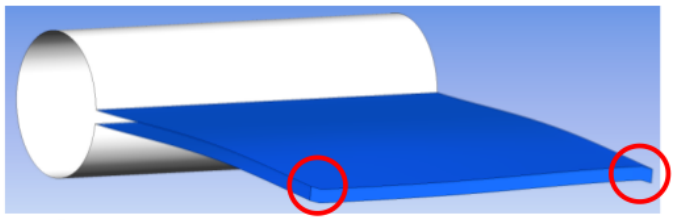

FIGURE 9: NON-PHYSICAL DEFORMATION OF RUBBER IN SPANWISE DIRECTION

4. CONCLUSION

In this work the SST-SBES model of Ansys (2017) is applied in the computation of a turbulent-FSI benchmark of De Nayer et al. Within the transient decoupled simulation the non-zonal hybrid RANS-LES model demonstrates a good performance, reflected in the prediction of the Strouhal number. In particular, a flow phenomenon, that is, transition in shear layer which is difficult to be reproduced by DES variants with their strategy in modifying the RANS length scale, can be demonstrated by SST-SBES due to the key role of the shielding function f_p in uniting the SST and WALE-LES models. On the LES grid resolution the shielding function f_p performs well to separate the RANS region with the LES area, and the demarcation line uniquely resembles the geometry. With these findings the hybrid formulation therefore is employed for the turbulent-FSI computation on the coarsened mesh.

In the FSI simulation, the turbulence scales interacting with the moving and deforming rubber immersed in the subcritical Reynolds number are successfully resolved by the non-zonal hybrid turbulence formulation on a coarsened mesh. Two crucial issues, on the other hand appear. The frequency of oscillation as well as the amplitude of displacement in the rubber deflection under-predicts the reference data. Secondly, the unphysical deformation of the rubber occurs in the spanwise direction. The choice of exponent c in the mesh stiffness model presumably contributes to this matter as the rubber interacts with the complex turbulence scales predicted by the hybrid approach, thus affecting the movement and deformation of the elastic structure which is controlled by the mesh stiffness. Accordingly a further investigation into modifications of the mesh stiffness formulation would be of interest. Concerning the LES component in SST-SBES, it would be advantageous for further research to consider another form of the SGS model that includes structure functions of velocity difference, such as the Ducros model [Ducros et al 1996] as an alternative to the WALE-LES methodology.

ACKNOWLEDGEMENTS

The author is grateful to Professor Dr. rer. nat Michael Schäfer who has trusted him with the research in turbulence and fluid-structure interaction at the Department of Numerical Methods in Mechanical Engineering, Technische Universität Darmstadt and gratefully acknowledges the supports of the Lichtenberg High Performance Computer of TU Darmstadt for extensive computations in the research and the scholarships of Kementerian Riset, Teknologi, dan Pendidikan Tinggi Republik Indonesia and Universitas Kristen Petra. It is expressly stated that major parts of this manuscript have been prepared by the author during his doctoral study at TU Darmstadt. Finally, insightful comments from reviewers that have strengthened the manuscript as well as discussions with Dr. -Ing. Benedikt Flurl of Ansys Germany, Mr. Martin Straka of Physikalisch-Technische Bundesanstalt Berlin, Dr.-Ing. Wolfgang Bauer of Ansys Germany and Institut für Land- und Seeverkehr – Fachgebiet Fahrzengantriebe of Technische Universität Berlin, and Abe H. Lee, Ph.D., graduate of the Pennsylvania State University, are also gratefully acknowledged.

REFERENCES

[1] A. Ali. “On the simulation of turbulent fluid-structure interaction.” Dr.-Ing. dissertation, Technische Universität Darmstadt, (2017).

[2] A. Islam, B. Thornber. A high-order hybrid turbulence model with implicit large-eddy simulation. Computers and Fluids, 167: 292-312 (2018).

[3] A. Kalmbach. “Experimental investigations on vortex-induced fluid-structure interaction benchmarks and corresponding RANS predictions.” Dr.-Ing. dissertation,

Helmut-Schmidt Universität/ Universität der Bundeswehr, (2015).
[4] A. Kondratyuk. “Investigation of the Very Large Eddy Simulation Model in the context of fluid-structure interaction.” Dr.-Ing. dissertation, Technische Universität Darmstadt, (2017).
[5] Ansys 17.2. *Ansys CFX-Solver Theory Guide*. Release 17.2. Ansys, Inc. Canonsburg, Pennsylvania (2017).
[6] C. Fureby, F. F. Grinstein. Monotonically integrated large eddy simulation of free shear flows. AIAA Journal, 37:544-556 (1999).
[7] D. Drikakis, M. Hahn, A. Mosedale, B. Thornber. Large Eddy Simulation using High-Resolution and High-Order Methods. Philosophical Transactions of the Royal Society of London, 367: 2985-2997 (2009).
[8] F. Ducros, P. Comte, M. Lesieur. Large-eddy simulation of transition to turbulence in a boundary layer developing spatially over a flat plate. Journal of Fluid Mechanics, 326: 1-36, (1996).
[9] F. Nicoud, F. Ducros. Subgrid-scale stress modelling based on the square of the velocity gradient tensor. Flow, Turbulence and Combustion, 62(3): 183-200 (1999).
[10] F. R. Menter. *Stress-Blended Eddy Simulation (SBES): A New Paradigm in Hybrid RANS-LES Modelling*. 6th HLRM Symposium, (France, 2016).
[11] F. R. Menter. Two-equation eddy-viscosity turbulence models for engineering applications. AIAA Journal, 32(8): 1598-1605 (1994).
[12] G. De Nayer, A. Kalmbach, M. Breuer. “Fluid-structure interaction in turbulent flow past cylinder/plate configuration I (First swiveling mode)”, last edited on 10 May 2018, http://www.kbwiki.ercoftac.org/w/index.php/Abstr:UFR_2-13
[13] H. P. S. Pratomo. Scale resolving simulations of coherent unsteadiness over a benchmark configuration at a subcritical Reynolds number. AIP Conference Proceedings, 2223: 1-10 (2020).
[14] J. Apelt, G. S. West. The effects of wake splitter plates on bluff-body flow in the range $10^4 < R < 5 \times 10^4$. Part 2, Journal of Fluid Mechanics, 71(1): 145-160 (1975).
[15] J. Smagorinsky. General circulation experiments with the primitive equations: I. The basic experiment. Monthly Weather Review, 91(3): 99-164 (1963).
[16] M. F. Alam, D. Thompson, D. K. Walters. “Critical assessment of hybrid RANS-LES modeling for attached and separated flows.” Turbulence Modelling Approaches: Current State, Development Prospects, Applications, K. Volkov, ed., IntechOpen, pp. 1-28, (2017).
[17] P. R. Spalart, W.-H., Jou, M. Strelets, S. R. Allmaras. Comments on the feasibility of LES for wings, and on a hybrid RANS/ LES approach. In: *Proceeding of the 1st AFOSR International Conference on DNS/ LES*. C. Liu, Z. Liu (Eds). Columbus: Greyden Press, pp. 137-147, (1997)
[18] T. Reimann. “Numerische Simulation von Fluid-Struktur-Interaktion in turbulenten Stroemungen”. Dr.-Ing. Dissertation, Technische Universitaet Darmstadt, (2013).
[19] Y. Xie, Y. Rao, W. Li, J. Qin. Experiments and Stress-Blended Eddy Simulations of turbulent flow over edge-rounded dimples. International Journal of Thermal Sciences, 154:1-15, (2020).

ASME-paper1

ORIGINALITY REPORT

18%	9%	16%	2%
SIMILARITY INDEX	INTERNET SOURCES	PUBLICATIONS	STUDENT PAPERS

PRIMARY SOURCES

1	Hariyo P. S. Pratomo. "Scale resolving simulations of coherent unsteadiness over a benchmark configuration at a subcritical Reynolds number", AIP Publishing, 2020 Publication	10%
2	read.pudn.com Internet Source	1%
3	www.e3s-conferences.org Internet Source	1%
4	asmedigitalcollection.asme.org Internet Source	1%
5	Submitted to University of Johannsburg Student Paper	<1%
6	www.intechopen.com Internet Source	<1%
7	link.springer.com Internet Source	<1%
8	Asiful Islam, Ben Thornber. "A high-order hybrid turbulence model with implicit large-eddy	<1%

	simulation", Computers & Fluids, 2018 Publication	
9	hal.archives-ouvertes.fr Internet Source	<1%
10	event.asme.org Internet Source	<1%
11	aip.scitation.org Internet Source	<1%
12	epdf.tips Internet Source	<1%
13	open.library.ubc.ca Internet Source	<1%
14	"Progress in Hybrid RANS-LES Modelling", Springer Science and Business Media LLC, 2020 Publication	<1%
15	Gary J. Brown, David F. Fletcher, Jeremy W. Leggoe, David S. Whyte. "Application of hybrid RANS-LES models to the prediction of flow behaviour in an industrial crystalliser", Applied Mathematical Modelling, 2020 Publication	<1%
16	repository.tudelft.nl Internet Source	<1%
17	mafiadoc.com	

	Internet Source	<1%
18	pericles.pericles-prod.literatumonline.com Internet Source	<1%
19	International Journal of Numerical Methods for Heat & Fluid Flow, Volume 26, Issue 5 (2016) Publication	<1%
20	SATOAKI OMORI. "Eddy Viscosity Calculation Along the Chemical Rocket Thrust Chamber Wall Using Turbulent Kinetic Energy", Combustion Science and Technology, 1973 Publication	<1%
21	Han, Xingsi, and Siniša Krajnović. "Validation of a novel very large eddy simulation method for simulation of turbulent separated flow : VALIDATION OF A NOVEL VLES FOR TURBULENT SEPARATED FLOW", International Journal for Numerical Methods in Fluids, 2013. Publication	<1%
22	Tristan Favre, Gunilla Efraimsson. "An Assessment of Detached-Eddy Simulations of Unsteady Crosswind Aerodynamics of Road Vehicles", Flow, Turbulence and Combustion, 2011 Publication	<1%

23	Asiful Islam, Ben Thornber. "Development and Application of a novel RANS and Implicit LES Hybrid Turbulence Model for Automotive Aerodynamics", SAE International, 2016 Publication	<1%
24	pastel.archives-ouvertes.fr Internet Source	<1%
25	arc.aiaa.org Internet Source	<1%
26	Tausif Jamal, D. Keith Walters. "A Dynamic Time Filtering Technique for Hybrid RANS-LES Simulation of Non-Stationary Turbulent Flow", Volume 2: Computational Fluid Dynamics, 2019 Publication	<1%
27	Michael A. Leschziner. "Computational Methods Combining Large Eddy Simulation with Approximate Wall-Layer Models for Predicting Separated Turbulent Near-Wall Flows", Frontiers of Computational Science, 2007 Publication	<1%
28	Wu, D.. "The transient flow in a centrifugal pump during the discharge valve rapid opening process", Nuclear Engineering and Design, 201012 Publication	<1%
29	178.250.48.185	

	Internet Source	<1%
30	Turnbull, J.. "Transient averaging to combine large eddy simulation with Reynolds averaged Navier-Stokes simulations", Computers and Chemical Engineering, 20050115 Publication	<1%
31	dspace.lib.cranfield.ac.uk Internet Source	<1%
32	"Quality and Reliability of Large-Eddy Simulations", Springer Science and Business Media LLC, 2008 Publication	<1%
33	Hariyo Priambudi Setyo Pratomo, Fandi Dwiputra Suprianto, Teng Sutrisno. "Preliminary Study on Mesh Stiffness Models for Fluid-structure Interaction Problems", E3S Web of Conferences, 2019 Publication	<1%
34	A.R. Donovan. "The potential to provide wide band data links to US Submarine Forces via DSCS SHF MILCOMSAT", Proceedings of MILCOM 93 - IEEE Military Communications Conference MILCOM-93, 1993 Publication	<1%
35	GM Stavrakakis, NM Tomazinakis, NC	<1%

Markatos. " Modified ‘closure’ constants of the Standard turbulence model for the prediction of wind-induced natural ventilation ", Building Services Engineering Research and Technology, 2011
Publication

36 "New Results in Numerical and Experimental Fluid Mechanics VIII", Springer Nature, 2013 <1%
Publication

37 "Progress in Hybrid RANS-LES Modelling", Springer Science and Business Media LLC, 2018 <1%
Publication

38 Han Li, Qiaogao Huang, Guang Pan, Xinguo Dong. "The transient prediction of a pre-swirl stator pump-jet propulsor and a comparative study of hybrid RANS/LES simulations on the wake vortices", Ocean Engineering, 2020 <1%
Publication

Exclude quotes	On	Exclude matches	< 5 words
Exclude bibliography	On		